

## Improving profile of multi-electrode Fresnel-type liquid crystal lens utilizing local control of pretilt angle

Il Hwa Jeong<sup>1</sup>, Ji Hoon Yu<sup>1</sup>, Young Jin Lim<sup>1</sup>, Ki Hoon Song<sup>1</sup>, Hongwen Ren<sup>1</sup>, Gi-Dong Lee<sup>2\*</sup>, and Seung Hee Lee<sup>1\*</sup>

<sup>1</sup>Applied Materials Institute for BIN Convergence, Department of BIN Fusion Technology, Chonbuk National University, Jeonju 561-756, Korea

<sup>2</sup>Department of Electronics Engineering, Dong-A University, Busan 604-714, Korea

E-mail: gdlee@dau.ac.kr; lsh1@chonbuk.ac.kr

Received March 4, 2014; accepted April 15, 2014; published online May 14, 2014

A multi-electrode driving Fresnel liquid crystal lenticular lens (MeD-Fresnel type LC lens) for switchable 2D/3D liquid crystal displays has been studied. The demonstrated lens which has fine-patterned electrodes only on one substrate, minimizing lens error by mis-assembly between top and bottom substrate, and uses a discontinuous non-uniform electric field with local control of surface pretilt angle by polymer stabilization technique, exhibits excellent lens profile compared with conventional lens without local control of pretilt angle.

© 2014 The Japan Society of Applied Physics

Recently, the applications of displays realizing three-dimensional (3D) images have been rapidly expanding worldwide. Many researchers have made efforts to develop the technologies that can switch from two-dimensional (2D) to 3D display with high brightness, and high resolution.<sup>1-5)</sup> Generally, the 3D technologies are classified into stereoscopic and auto-stereoscopic types. Stereoscopic 3D is the most popular approach at present because of its rather easy fabrication. However, one of the major disadvantages of stereoscopic displays is that viewers feel uncomfortable because of wearing the glasses. As a comparison, auto-stereoscopic displays have been studied because of glasses free. In the auto-stereoscopic 3D displays there are two main methods for 3D imaging; barrier type<sup>6)</sup> and microlens array type.<sup>7)</sup> Barrier type is easier to manufacture than the lens type. However, the barrier type has a serious disadvantage of reducing brightness in 3D image. As a consequence, nowadays, many researchers have been studying the microlens-based 3D display using a liquid crystal (LC) because the display has some advantages such as minimum loss of brightness and usefulness for 2D/3D switchable display. To make the 2D/3D switchable display, two main methods exist: polarization-sensitive polymeric lens with polarization switchable LC cell<sup>2)</sup> and LC graded-refractive-index lens (LC GRIN).<sup>8-10)</sup> For LC GRIN lens, LC molecules orient with different orientation angles according to spatially distributed electric field to form graded-refractive index profile. The major characteristic of LC GRIN lens is the thick cell gap which can be as thick as  $\sim 60$  to  $70 \mu\text{m}$  due to the limited optical anisotropy in refractive index ( $\Delta n$ ) of LC. As a result, the LC GRIN lens has a very slow switching time. Therefore, decreasing the switching time of the LC lens is necessary. In addition, a gap spacer which keeps such a high cell gap appears noticeable to naked eyes as a defect so that reducing cell gap would allow to use the spacer with smaller size which does not affect the image quality of the display.

As a perfect solution overcoming abovementioned problems, the multi-electrode driving Fresnel LC lens (MeD-Fresnel) with a narrow cell gap has been proposed.<sup>11-13)</sup> In these approaches, fine patterned electrodes exist on top and bottom substrates and a set of different voltages is applied to each electrode to generate graded-refractive index profile. Nevertheless, the boundary profile of the previous MeD-Fresnel LC lens is very difficult to achieve so that MeD-Fresnel LC lens profile and ideal Fresnel lens profile still

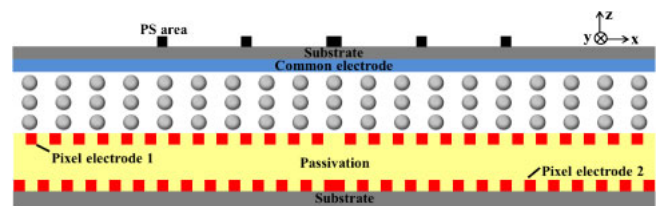


**Fig. 1.** (Color online) Structure of multi-electrode driving Fresnel LC Lens in which patterned pixel electrode 1 and 2 exists on bottom substrate and non-patterned common electrode exists on top substrate. The black areas on top substrate indicate locations for polymer stabilization.

have some mismatches.<sup>14,15)</sup> In addition, the mismatch becomes severer when top and bottom substrates for the lens are misaligned.

To solve these problems, we have studied MeD-Fresnel LC lens in which fine patterned electrodes exist only on bottom substrate to minimize the mismatch due to mis-assembly between top and bottom substrates and polymer stabilization (PS) technology of reactive mesogen (RM) to control pretilt angle of LC locally is applied to achieve better lens profile.

The proposed electrode structure for MeD-Fresnel LC lens is illustrated in Fig. 1. Common electrode without patterning exists on top substrate and signal electrodes exist on bottom substrate in which two different and fine-patterned transparent electrodes, indium-tin-oxide (ITO) exist with passivation layer between them. In each electrode, a different set of voltage is applied to generate different LC molecular orientation angle for ideal MeD-Fresnel lens. In our studies, pitch of the LC lens is  $216 \mu\text{m}$  and the fine-patterned ITOs have electrode width of  $4 \mu\text{m}$  width and spacing of  $4 \mu\text{m}$  except that the width of the center electrode in the first ITO layer is  $8 \mu\text{m}$ . The thickness of passivation layer ( $\text{SiN}_x$ , dielectric constant: 6.5, refractive index: 1.5) between the two electrode layers is  $0.6 \mu\text{m}$  and the cell gap ( $d$ ) is  $15 \mu\text{m}$ . The LC used in this study has physical properties such as dielectric anisotropy  $\Delta\epsilon = 6.6$ , high birefringence  $\Delta n = 0.2294$  at  $550 \text{ nm}$ , and three elastic constants  $K_{11} = 9.7 \text{ pN}$ ,  $K_{22} = 5.2 \text{ pN}$ , and  $K_{33} = 13.3 \text{ pN}$ . The LCs are homogeneously aligned with its optic axis along  $y$ -direction and surface tilt angle of  $4^\circ$  over whole area.

We modeled the field-dependent LC reorientation and its refractive index distribution with the commercially available software Techwiz LCD (Sanayi System) while optimizing an

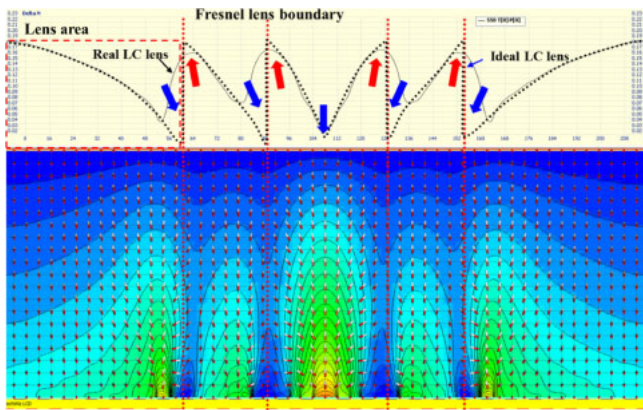


**Fig. 2.** (Color online) Simulation result of refractive index distribution of Fresnel LC lens (dotted line) compared with ideal Fresnel lens (solid line) with LC director profile and the electric potential energy distribution in MeD Fresnel LC lens. The profile of proposed lens does not match ideal lens. The rectangular area with dotted line and vertical dotted lines indicate domains for lens and lens boundary, respectively.

applied voltage to each electrode. Many different sets of voltages applied to each electrode which controls LC orientation locally were tried and the retardation profile obtained through optimization is shown in Fig. 2. As indicated, ideal Fresnel lens profile has an abrupt change in retardation profile to have a lens boundary. In order to achieve such an abrupt change in LC orientation at the lens boundary, maximum (7 V) and minimal (0 V) voltage at two neighboring electrodes should be applied to have almost vertical and homogenous LC orientation respectively. With such a profile, a linearly polarized light propagating along the  $y$ -direction experiences minimal and maximal refractive index (optical paths) at two neighboring electrodes, forming lens boundary. In other words, only vertical electric field ( $E_z$ ) is required to control LC orientation. However, such large voltage difference between two electrodes generates fringe electric field and the horizontal electric field ( $E_x$ ) component of the fringe field near bottom substrate causes twist deformation of LC molecules. Then the twist deformation between two electrodes and the following collective motion of LC molecules disturb continuous vertical and homogenous LC alignment at lens boundary. Consequently, the lens profile obtained by proposed cell structure and optimized driving conditions could not match the ideal Fresnel lens profile, especially profile of lens boundary, as clearly indicated in Fig. 2. Therefore, suppressing or increasing optical path as indicated by arrows at the lens boundary is required to match ideal lens, which is critical factor determining crosstalk in 3D display using the lens.<sup>16,17)</sup>

In the proposed lens, the LC is homogeneously aligned in an initial state so that achieving a perfect vertical orientation is very difficult due to residual homogeneously aligned LC at both surfaces by strong anchoring. Therefore, if we can control initial surface pretilt angle locally such that a relatively high surface tilt angle is given at the position where vertical orientation is required, better lens boundary can be achieved. Controlling surface pretilt angle locally is challenged by doping RM into LC mixtures and then UV irradiation to the cell while a proper voltage is applied to each electrode.

In order to realize different surface pretilt angle locally, 2 wt % of photopolymerizable RM257 from Merck RM257

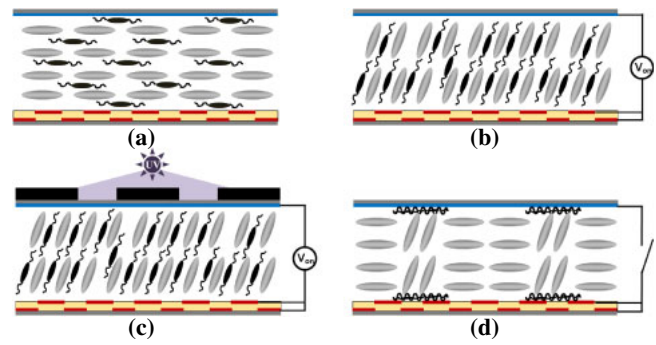


**Fig. 3.** (Color online) Schematic drawings of controlling pretilt angle locally via polymer stabilization process: (a) the mixture is homogeneously aligned, (b) the vertical field is applied to the cell, (c) the UV is exposed to the lens boundary via UV mask, and (d) high surface tilt angle is formed at the lens boundary even after the voltage is released.

with respect to LC mixture and a 0.01 wt % of photoinitiator (Irgacure 651) with respect to RM are mixed with host LC (Merck MAT 10-556). The physical properties of the LC are the same as those given in the simulations. The mixture is filled into the homogeneously aligned cell with the same electrode structure used in the simulation so that the LC and RM is aligned uniformly, as shown in Fig. 3(a). Once the uniform alignment is confirmed under polarizing optical microscope (POM), the vertical electric field is applied to the cell so that the LC reorients along the vertical direction [see Fig. 3(b)]. Then UV ( $1.3 \text{ mW/cm}^2$  at 365 nm for 2000 sec) is exposed to the cell via UV mask, in which UV is only exposed to the lens boundary where an abrupt change in refractive index is required [see Fig. 3(c)]. Finally, we expect the exposed area has a high surface pretilt angle even after the applied voltage is released to zero because the LC director with a high tilt angle is fixed by polymerized RM, as described in Fig. 3(d).

In experiments, the opened areas of the mask has diameter of  $8 \mu\text{m}$  at the center and  $4 \mu\text{m}$  at both sides of center. After UV exposure to the cell, POM images are observed as proof of formation of high surface tilt angle at the lens boundary, as shown in Fig. 4. Since the LC is homogeneously aligned in the initial state, high surface tilt angle at the lens boundary would cause reduced retardation ( $d\Delta n$ ). As a result, POM image shows clearly decreased transmittance at the lens boundary compared with that in other areas at 0 V [see Fig. 4(a)] and when the applied voltage between top and all bottom electrodes increased to 10 V, the LC director aligns along vertical direction so that the transmittance decreases in all areas while the transmittance change at the center of the lens is negligible [see Fig. 4(b)]. From POM images as a function of applied voltages and retardation measurements, surface pretilt angles in the dark regions were found to be about  $90^\circ$  and  $73^\circ$  at the center and the other positions, respectively, confirming control of pretilt angles locally. The light intensity across the  $x$ -axis of the microscope images also confirmed the existence of pretilt angle locally such that the light intensity at the center of lens was lower than other positions, as shown Fig. 4(c). Nevertheless, we found that even the area without UV exposure also shows some level of decreased transmittance, which is associated with diffraction effects of UV mask partly and also with diffusion of RM with

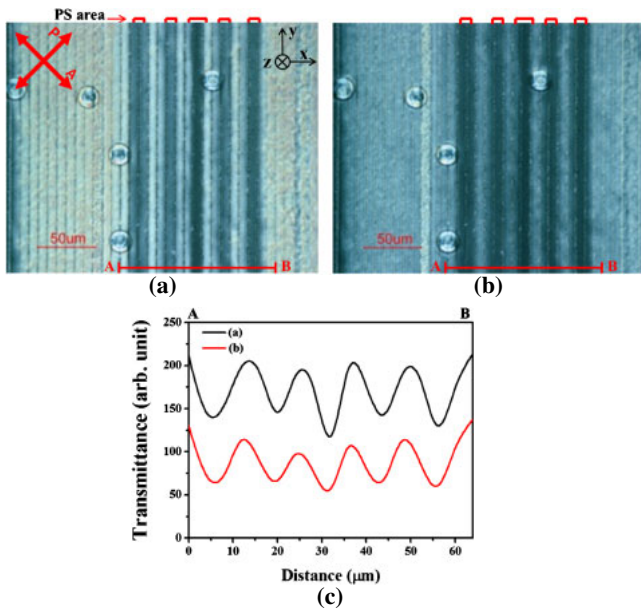


**Fig. 4.** (Color online) Observed polarizing optical microscope image after polymer stabilization of surface pretilt angle at the lens boundary: (a) 0 V and (b) 10 V. The light intensity across the  $x$ -axis of the microscope images along the line AB also confirms the existence of pretilt angle locally (c). Here P and A indicate polarizer and analyzer, respectively and five circles in the images are plastic ball spacers to keep the cell gap.

polymerization during UV exposure partly. We believe more precision control of mask size, process and optimization of RM related materials would improve this problem.

Once the feasibility of local control of surface pretilt angle is confirmed, a simulation is performed again assuming surface pretilt angle of  $90^\circ$  at the lens boundary, as shown in Fig. 5. In the normal MeD-Fresnel LC lens, the refractive index profile could not match the ideal lens profile. However, the lens profile with local control of pretilt angle presents remarkable improvement in the refractive index distribution compared with the former case. In order to quantify the matching levels of LC lens to the ideal Fresnel lens, an error function (EF)<sup>15)</sup> is defined as

$$EF = \sqrt{\frac{\sum_{i=0}^R (S_i - P_i)^2}{R}} \times 100 (\%) \quad (1)$$

where  $S_i$  is the refractive index distribution of simulated Fresnel LC lens,  $P_i$  is the refractive index distribution of ideal Fresnel lens, and  $R$  is the aperture size represented the lens pitch. In order to find out the effect of local control of pretilt angle, EF in lens profile (lens error) and lens boundary (Fresnel error) is calculated, as indicated in Table I. The lens error seems to be slightly worse in the improved structure but the Fresnel error which is a critical factor determining the level of crosstalk in 3D display decreases from 35.0 to 16.9% and thus the overall EF also significantly decreases from 35.5 to 18.4%.

Summarizing our studies, we studied a MeD-Fresnel LC lens with thin cell gap of  $15 \mu\text{m}$  which is very useful in switchable 2D/3D display. In the lens, strong fringe electric field between patterned electrodes and collective behavior of LC, the refractive index distribution of MeD-Fresnel LC

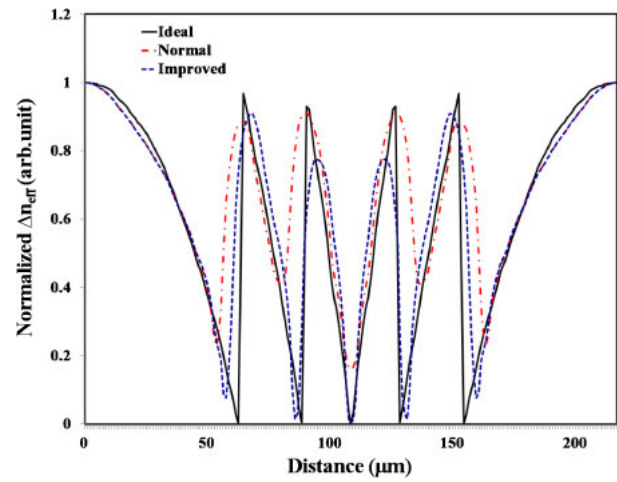


**Fig. 5.** (Color online) Simulation result of refractive index distribution of Fresnel LC lens through PS process compared with simulation result of Fresnel LC lens without PS and ideal Fresnel lens.

**Table I.** Calculated error function of MeD-Fresnel lens in conventional and proposed device in %. Lens error and Fresnel error represent level of mis-matching in lens domain and Fresnel lens boundary between ideal lens and proposed lens, as indicated in Fig. 2.

	All area error	Lens error	Fresnel error
Normal	35.5	5.7	35.0
Improved	18.4	7.2	16.9

lens does not perfectly match with that of ideal Fresnel lens, resulting in a severe crosstalk. In order to overcome such an intrinsic problem, control of surface pretilt angle locally is performed and then the lens profile is greatly improved, allowing the proposed concept to be applicable future LC tunable lens with thin cell gap for switchable 2D/3D display.

**Acknowledgements** This work was supported by LG Display and the National Research Foundation (NRF) Korea, the Korea–China Joint Research Program under Grant No. 2012-0004814.

- 1) H. K. Hong, S. M. Jung, B. J. Lee, H. J. Im, and H. H. Shin, *SID Symp. Dig. Tech. Pap.* **39**, 348 (2008).
- 2) G. J. Woodgate and J. Harrold, *SID Symp. Dig. Tech. Pap.* **34**, 394 (2003).
- 3) S. H. Lee, S. L. Lee, and H. Y. Kim, *Appl. Phys. Lett.* **73**, 2881 (1998).
- 4) S. H. Lee, S. H. Hong, H. Y. Kim, J. H. Park, and W. G. Lee, *SID Symp. Dig. Tech. Pap.* **31**, 763 (2000).
- 5) H. J. Yun, M. H. Jo, I. W. Jang, S. H. Lee, S. H. Ahn, and H. J. Hur, *Liq. Cryst.* **39**, 1141 (2012).
- 6) W. L. Chen, F. H. Chen, and C. H. Tsai, *Proc. 11th Int. Meet. Information Display*, 2011, p. 474.
- 7) H. Ren, Y. H. Fan, and S. T. Wu, *Appl. Phys. Lett.* **83**, 1515 (2003).
- 8) S. Sato, *Jpn. J. Appl. Phys.* **18**, 1679 (1979).
- 9) B. Wang, M. Ye, and S. Sato, *Appl. Opt.* **43**, 3420 (2004).
- 10) M. Ye and S. Sato, *Jpn. J. Appl. Phys.* **41**, L571 (2002).
- 11) H. Ren, S. Xu, and S.-T. Wu, *Opt. Express* **20**, 26464 (2012).
- 12) Y. H. Fan, H. W. Ren, and S. T. Wu, *Opt. Express* **13**, 4141 (2005).
- 13) J. G. Lu, X. F. Sun, Y. Song, and H. P. D. Shieh, *J. Disp. Technol.* **7**, 215 (2011).
- 14) Y. P. Huang, L. Y. Liao, and C. W. Chen, *J. Soc. Inf. Disp.* **18**, 642 (2010).
- 15) Y. P. Huang, C. W. Chen, and T. C. Shen, *SID Symp. Dig. Tech. Pap.* **40**, 336 (2009).
- 16) S. Oka, T. Sugita, T. Naganuma, T. Saito, S. Komura, and T. Miyazawa, *SID Symp. Dig. Tech. Pap.* **43**, 387 (2012).
- 17) Y.-Y. Kao and P. C.-P. Chao, *SID Symp. Dig. Tech. Pap.* **42**, 13 (2011).